Project Study: Tracking Drone Orientation with Multiple GPS Receivers

Zhan Zhang, *Student Member, IEEE,* and Danni Wu, *Student Member, IEEE*

I. Introduction

WITHOUT a good awareness of orientation and balance, a drone cannot effectively controll its rotors to achieve desired flying status. A natural response is to install redundant inertial measurement units (IMU). IMU is an electronic device that measures and reports a body's specific force, angular rate, and the magnetic field surrounding the body, using a combination of accelerometers and gyroscopes, sometimes also magnetometers.

IMUs are typically used to maneuver aircraft, including unmanned aerial vehicles (UAVs), among many others, and spacecraft, including satellites and landers. Recent developments allow for the production of IMU-enabled GPS devices.

An IMU allows a GPS receiver to work when GPS-signals are unavailable, such as in tunnels, inside buildings, or when electronic interference is present. Unfortunately, redundancy only addresses unreliable hardware. Various noise sources, including motor vibration, electromagnetic interference, and ambient ferromagnetic influences, create unreliablity for the IMU. Worse even, the errors would accumulate through time and the IMUs are prone to various types of correlated failures.

The SafetyNet is a fail-safe mechanism for IMU failures. The basic idea is using multiple GPS to track 3D orientation of the UAV. The SafetyNet design includes 4 GPS receivers at four arms of the single drone upon IMU failure, we utilize these GPS receivers to estimate the drones 3D orientation. As an alternative to the IMUs, SafetyNet uses GPS signals to estimate the real time orientation of the drone without any inertial or magnetometer assistance. Chanllenge comes that the traditional GPS system iccurs an error around 2 3 meters and the more advanced Differential GPS technology would still have a relative error in the scale of 10 20 centimeters (which equals to 20 degree in orientation). However, opportunities exist in relative GPS signal information and we aim to utilize the spatio-temporal information to achieve better accuracy.

The core additions of the SafetyNet, can be distilled as follows:

- Manipulating measurements across pairs of GPS receivers, satellites, and consecutive time points, capture 3D orientation from two different perspective, which can institute transition model and measurement model of Kalman filter.
- GPS carrier-phase measurements can be used to achieve very precise positioning solutions. Carrier-phase measurements are much more precise than pseudorange measurements, but they are ambiguous by an integer number of cycles. GPS phase measurements are composed of an unknown portion, called integer ambiguity. In attempting to resolve this ambiguity, past work have adopted techniques akin to hard decoding, where the most likely state-estimate is propagated across time. We design the equivalent of soft decoding, whereby top-K possibilities of the ambiguity are propagated, each associated with an inferred probability. A particle filter is used to execute this idea the particle filter degenerating back into the Kalman Filter when the ambiguity is resolved confidently.
- We break away from the classical particle filter approach and adjust the state of the particles based on available measurements. This speeds up convergence of the system, while requiring fewer particles (considerably reducing the computational complexity). As a result, the overall SafetyNet system lends itself to real time operation on todays drone hardware.

II. Problem Formulation

A. Drone Model

In this study, the drone is modelled with 4 GPS receivers installed on its 4 arms with a distance of 10 centimeters to the center. Therefore, a baseline matrix is generated as shown in figure 1 to model the ground truth relation between different receivers at different states.

The baseline matrix has the form:

$$B = \begin{bmatrix} \rho_{41} & \rho_{42} & \rho_{43} \end{bmatrix} \tag{1}$$

where ρ_{ij} is the vector between receiver i and j

$$\rho_{ij} = \rho_i - \rho_j \tag{2}$$

Z. Zhang and D. Wu was with the Department of Electrical and Computer Engineering, Cornell Tech

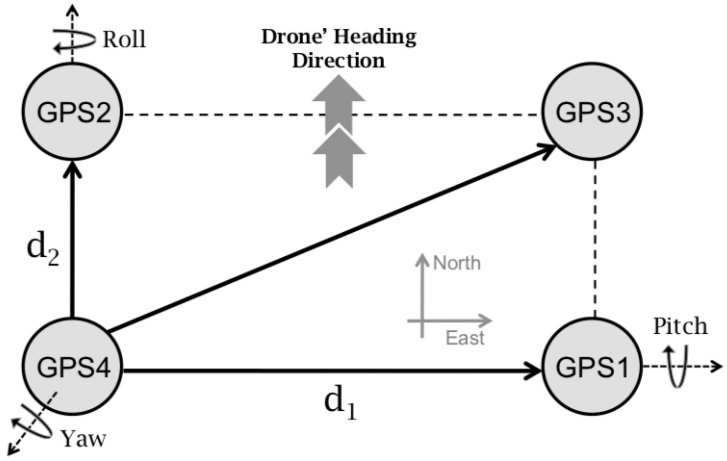

Fig. 1: Baseline Matrix

B. Pseudorange

Generally, the GPS operates in measuring the the time difference between transmitter and receiver and the Pseudorange, which is the estimated distance between both ends is formed as in equation 3.

$$Pseudorange = ToF * c \tag{3}$$

where ToF is the time difference and c represents the speed of light.
However, when a satellite transmits a signal, it includes clock error as the starting time of transmission is obtained from its atomic clock. The reception time of the ground receiver is also recorded by less accurate local clock. Because the clock of a typical GPS receiver is not synchronized to the GPS satellites. The resulting error can be up to 300 km. GPS signal can get delayed when it enters the Earths atmosphere because of refractions in the Ionosphere and Troposphere. When signal passes through a multipath channel, more errors would be introduced. In our study, we model the error in pseudorange at receiver i from the satellite s as in equation 4.

$$Pseudorange_i^s = \rho_i^s + ct_i - ct^s + A^s + M_i + \epsilon_i^s \tag{4}$$

Here, ρ_i^s represents the real range, t_i and t^s stand for the clock error at the receiver and transmitter sides correspondingly. A models the interference by the atmosphere, M_i stands for the multipath interference and ϵ_i^s represents the hardware noise in measuring.
The operation error from the system would be as large as 1-4 meters which is far from satisfaction. Therefore, the Differential GPS technology is introduced leveraging the difference in signal phase and highly improves the system accuracy.

C. Differential GPS

The differential GPS technology leverages the phase of received GPS signals to improve the accuracy. One advantage of carrier phase is that its changes over time can be tracked reliably by utilizing the doppler shift in the signals.
The phase model is shown in equation 5 by ignoring the multipath and hardware noise error.

$$\lambda\phi_i^s = \rho_i^s + ct_i - ct^s + A^s - N_i^s \tag{5}$$

where N_i^s is the number of full wavelengths in the range which we could not solve from the phase measurement. The unknown property of N_i^s is called as "integer ambiguity" and estimating the integer ambiguity is one of our major concern in the SafetyNet implementation. More discussion on integer ambiguity would come in later sections.
Environmental error sources in Equation 3 are correlated over short time periods and within small geographical areas (200 km). Thus, two GPS measurements across time can be subtracted (or differenced) to eliminate some of these factors. Similarly, simultaneous measurements from multiple GPS receivers can also be differenced. [29] This study propose 4 kind of differentials.

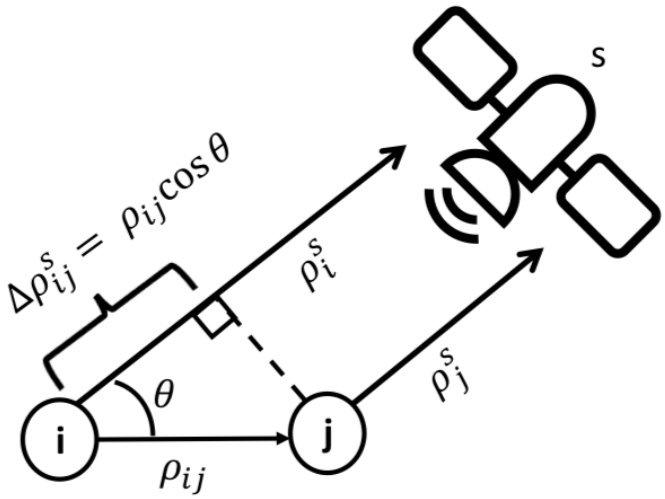

Fig. 2: $\lambda \triangle \phi^s_{ij} = \rho_{ij} \cdot \hat{l}_s + c \triangle t_{ij} - \lambda N_{ij}$

1) Single Differential across Receivers ($SD^s_{ij}(t)$):

$$\begin{aligned} \lambda \triangle \phi^s_{ij} &= \phi^s_i - \phi^s_j \\ &= \triangle \rho^s_{ij} + c \triangle t_{ij} - \lambda N_{ij} \end{aligned} \tag{6}$$

By differencing the phases at different receivers, correlated error sources of atmospheric delays and satellite clock biases disappear.

For further simplification, $\triangle \rho^s_{ij}$ is replaced by $\rho_{ij} \cdot \hat{l}_s$, where ρ_{ij} is the vector between two receivers and $\hat{l}_s$ is the line-of-sight unit vector from the receiver to the satellite. The transformation relationship is shown in figure 2.

The equation then become:

$$\lambda \triangle \phi^s_{ij} = \rho_{ij} \cdot \hat{l}_s + c \triangle t_{ij} - \lambda N_{ij} \tag{7}$$

2) Double Differential across Receivers and Satellites ($DD^{sk}_{ij}(t)$):

$$\begin{aligned} \lambda \bigtriangledown \triangle \phi^{sk}_{ij} &= \lambda \triangle \phi^s_{ij} - \lambda \triangle \phi^k_{ij} \\ &= \rho_{ij} \cdot (\hat{l}_s - \hat{l}_k) - \lambda \bigtriangledown \triangle N^{sk}_{ij} \end{aligned} \tag{8}$$

With the double differential, the clock error is further removed and the absolute orientation is achieved, but polluted by integer ambiguity. In this study, the spatio double differential forms our measurement model in the filtering process.

3) Single Differential across Time ($SD^s_i(t_{12})$): Similar to differentials across receivers and satellites, we can also perform differentials across time for the same receiver.

$$\lambda \triangle \phi^s_i(t_{12}) = \rho_i(t_{12}) \cdot \hat{l}_s + c t_i(t_{12}) \tag{9}$$

4) Double Differential across Receivers and Time ($DD^s_{ij}(t_1 t_2)$): By taking the difference between the two single differentials across time, we achieved a measurement the change in orientation, totally unpolluted by integer ambiguity. This measurement forms the system transition model in the filtering process.

$$\begin{aligned} \lambda \bigtriangledown \triangle \phi^s_{ij}(t_{12}) &= \lambda \triangle \phi^s_i(t_{12}) - \lambda \triangle \phi^s_j(t_{12}) \\ &= (\rho_{ij}(t_1) - \rho_{ij}(t_2)) \cdot \hat{l}_s + c \triangle t_{ij}(t_{12}) \end{aligned} \tag{10}$$

III. System Model

With both the temporal and spatial differentials, we are able to model the orientation estimation problem by forming the transition state and absolute measurements. The system diagram is provided in figure 3.

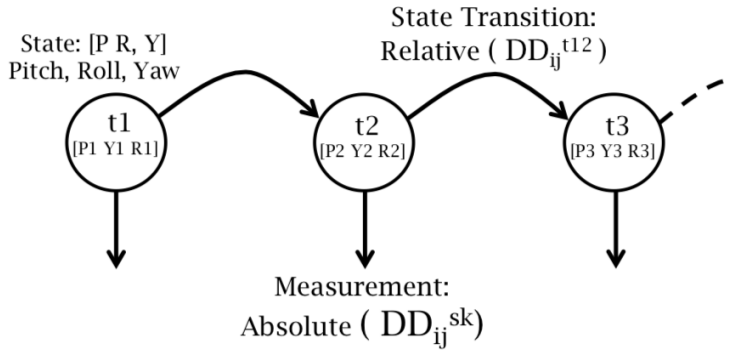

Fig. 3: System Model

1) Transition State: The temporal differential provides an accurate estimation upon the transition state as the integer ambiguity is cancelled. By minimizing the relative clock error, we can solve the equation to track the orientation change δq between states. Here we introduced the 3-dimensional vector representation of orientation $\delta\theta$ whose magnitude is the angle it rotates and direction is the axis it rotates around. By changing the representation metric, we are able to get rid of the constraint from quaternion and the estimation becomes a simple Least Square problem:

$$\lambda \bigtriangledown \triangle\phi_{ij}^{s}(t_{12}) = \rho_{ij}(q_0)[A(q_1)\hat{l}_s]_\times \delta\theta + c \triangle t_{ij}(t_{12}) \tag{11}$$

where $A(q)$ is the rotation matrix corresponding to the quaternion.
The solved $\delta\theta$ cannot be directly applied for transition state as the computation of rotation vector is not immuteable in large scale. We convert it back to quaternion form and the transition state becomes:

$$q_{k+1} = \delta q \bigotimes q_k \tag{12}$$

2) Absolute State: The spatial differential is transformed as our absolute measurement at each state.

$$\lambda \bigtriangledown \triangle\phi_{ij}^{sk} = \rho_{ij} \cdot (\hat{l}_s - \hat{l}_k) + \lambda \bigtriangledown \triangle N_{ij} \tag{13}$$

We can transform the measurement to a function of last state quaternion and a change in orientation in the vector form.

$$\lambda \bigtriangledown \triangle\phi_{ij}^{sk} - \rho_{ij}(q_0)A(q_n) \cdot (\hat{l}_s - \hat{l}_k) = \rho_{ij}(q_0)[A(q_n) \cdot (\hat{l}_s - \hat{l}_k)]_\times \delta\theta + \lambda \bigtriangledown \triangle N_{ij} \tag{14}$$

The measurement form would be further transformed in Extended Kalman Filter section for system linearization.

IV. Algorithms

A. Extended Kalman Filter

Referring back to equation 12, the transition function is intrinsically a nonlinear operation (the quaternion multiplication), we make linearized approximations using Extended Kalman Filter (EKF). Now, linearizing transition model around the estimated rotation vector associated with quaternion q_k by applying Taylor Expansion, we have:

$$\delta\theta_{k+1} = F\delta\theta_k + \omega_k \tag{15}$$

where ω_k is the system noise.
With the linearization process, the absolute state is transformed from absolute rotation in form of quaternion to change in rotation vector ($\delta\theta$), as the rotation vector has the property of having muteable operation in small scales and removes the constraint in magnitude.
As with the transition function above, the measurement function can be written in the following form:

$$y_{k+1} - y_0 = H\delta\theta_{k+1} + v_{k+1} \tag{16}$$

where:

$$y = \lambda \bigtriangledown \triangle\phi_{ij}^{sk} - \lambda \bigtriangledown \triangle N_{ij} \tag{17}$$

$$y_0 = \rho_{ij}(q_0)A(q_n) \cdot (\hat{l}_s - \hat{l}_k) \tag{18}$$

$$H = \rho_{ij}(q_0)[A(q_n) \cdot (\hat{l}_s - \hat{l}_k)]_\times \tag{19}$$

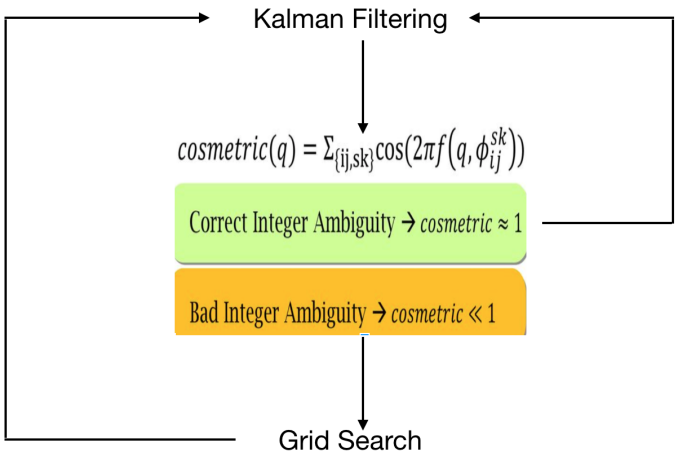

Fig. 4: Kalman Filter

and v_{k+1} is the measurement noise.
The transition model and measurment model can now be combined using an Extended Kalman Filter for a refined estimate of θ^{k+1}.
In the measurement model, the integer ambiguity still exists. Here we make the assumption that the integer ambiguity is already solved such that we can ignore it for the filtering process and come back to it afterwards.
Once the drone is flying, additional multiples of wavelengths can also accumulate, called cycle slips. This paper first describe ways to mitigate the initial N and discuss cycle slips thereafter.
Therefore, this paper did not measure integer ambiguity directly, but make it as an index to identify the estimation they got is correct or not. Their core intuition is to compute a Cos function on the value of $2\pi N_{ij}^{sk}$, since N_{sk} should be an integer, $Cos(2\pi N_{sk}^{ij})$ should equal to 1.
The process of Kalman filtering is listed as below:

- Using transition model to get estimation of the next time point: $\delta\theta_{k+1}$.
- Using measurement model to get the estimation of integer ambiguity. In an ideal case, the correct q should make the corresponding values of N_{ij}^{sk} equal to 1.
- Identify the correctness of integer ambiguity using the summation of cosmetrics:

$$M(q) = \sum_{ij,sk} cos(2\pi N_{sk}^{ij}) \tag{20}$$

  and compare $M(q)$ to the number of possible conbination pairs of receivers i, j and satellites s, k. If $M(q)$ approximates the number we consider it as correct and incorrect elsewise.
- If the integer ambiguity is correct, we can continue using kalman filter to estimate the state.
- If the integer ambiguity is not correct, the problem is transformed into a maximization problem. The cosmetric value would always be less than 1 if the estimated integer ambiguity is not an integer so our intention goes to find the best q to maximize $M(q)$, i.e.:

$$q_{coarse} = \underset{q}{\operatorname{argmax}}\, M(q) \tag{21}$$

- We simply perform a naive grid search in all 3 dimensions of ruler angle (yaw, pitch and roll) with a 5 degree step to find the optimized solution q_{coarse} to maximize the cosmetric value.
- After maximization, we update the previous q with q_{coarse}, and go back to step 2.

The system diagram is shown in figure 4.

B. Advanced Particle Filter

there exists one phenomenon called cycle slips, A cycle slips causes a jump in carrier-phase measurements when the receiver phase tracking loops experience a temporary loss of lock due to signal blockage or some other disturbing factor. It usually happens with highly aggressive flight drone. The process is listed as follows:

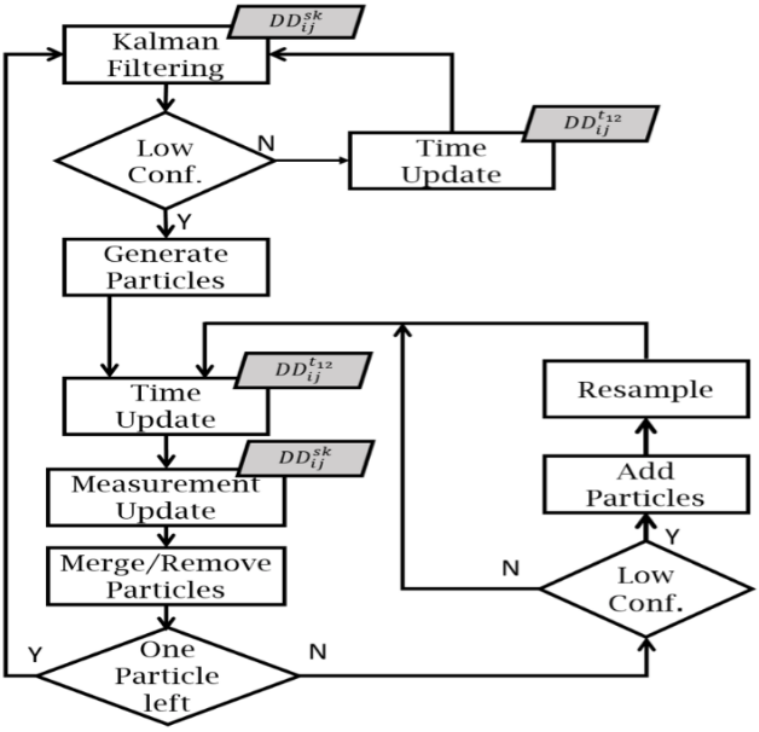

Fig. 5: Adjusted Particle Filter

- Using kalman filtering, we can calculate the cosmetric of each q_i
- if the cosmetric is lower than one, which means the confidence is verified as low, we switch from kalman filter to particle filter to solve the integer ambiguity problem. We select K values of orientation q the values whose corresponding Cos metric ranks in the top-K. We initialize K particles(from grid search with the top k confidence in cosmetric form) at each of these orientation states and update them via the transition model and measurement model.
- All things goes well, however, there is one problem of the slow convergence of particle filter. To solve this, this paper develope one advanced particle filter. In simple particle filter, we propagate to the next stage by transition model,and we weight them by the measurement model, and assign probability for later use for filtering and so on. This paper make a simple modification, they move the particle to a state that maximizes the likelihood,and then perform the resampling step. Thus, the net outcome is faster convergence for the correct ambiguities, while disappearing particles for incorrect ambiguities.
- Upon its convergence, and if the cosmetric close to 1, we switch back to Kalman filter again. If the cosmetric is much lower than 1,more particles are added and resampled resampling is performed such that the resulting particles are an equal mix of the (highest weighted) current and new particles, and continuing the particle filtering process until the cosmetric close to one, and we go back to step one.

The system diagram is shown in figure 5.

V. Simulation

A. Drone Simulation Platform

The simulation of the base drone is done based on Hector Quatercopter, an open-source implementation based on Robot Operation System (ROS) and Gazebo. The platform is shown in figure 6.

Ground truth data of the location and orientation data is collected to simulate the multiple GPS receivers attached to the drone. 4 GPS receivers are simulated on the 4 arms of the drone, rotated according to the ground truth orientation and shifted to the real location.

Two satellites are fixed on the Medium Earth Orbit and the phases are simulated from the corresponding distance between the satellite and the receiver.

As the drone's movement is relatively ignorable comparing to the distance to the satellites, the line-of-sight vector is considered as constant.

The Kalman and Adjusted Particle filters are performed on the simulated data.

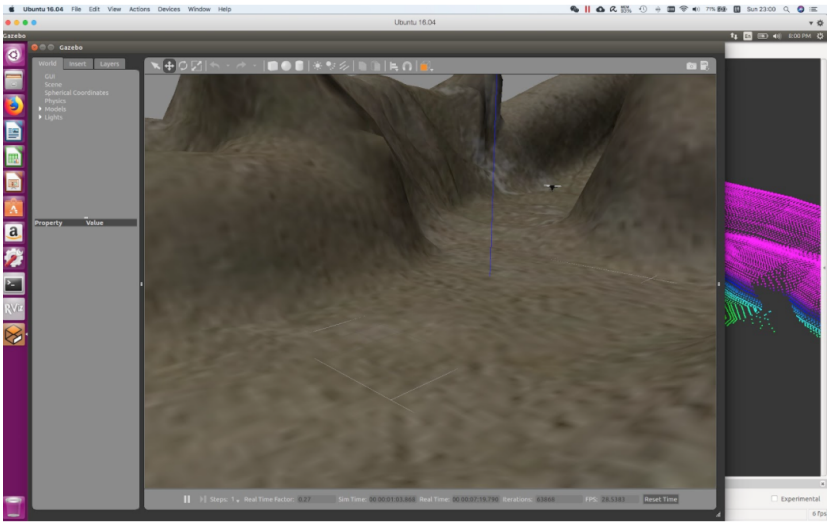

Fig. 6: Hector Quatercopter Simulation Platform

VI. Real World Applications

With the booming applications with unmanned autonomos vechicle, reliable orientation estimation has been a nontrivial concern. SafetyNet proposes the novel algorithm to track the orientation with multiple GPS receivers to promise an error of 2 degrees in environment where magnetic interference and acceleration error accumulates.
The reliablity and the accuracy of SafetyNet make it suitable in two major areas of applications.

a) Reliablity: in the estimation makes it suitable for large quatercopters in aggressive flying status and in highly interfered magnetic field. Typical applications include flying in urban area (interference in magnetic field), obstacle avoidance in high speed flight (error in accelerometers), etc.

b) Accuracy: in orientation estimation powers up the accuracy in autonomos controll algorithms. For example, accurate tracking of the camera pose make it possible to achieve better vision-based antonomos flying. 3D reconstruction from the drone's lens is another application benefits from the accuracy.

VII. Conclusion

The conclusion goes here.

References

[1] H. Kopka and P. W. Daly, *A Guide to LaTeX*, 3rd ed. Harlow, England: Addison-Wesley, 1999.